Journal of Luminescence 217 (2020) 116783

Contents lists available at ScienceDirect

Journal of Luminescence

journal homepage: http://www.elsevier.com/locate/jlumin

Thermoluminescence and defect centers in β-$CaSiO_3$ polycrystal

Carlos D. Gonzales-Lorenzo [a,**], T.K. Gundu Rao [a], Nilo F. Cano [b,*], Betzabel N. Silva-Carrera [c], René R. Rocca [b], Edy E. Cuevas-Arizaca [a], Jorge S. Ayala-Arenas [d,***], Shigueo Watanabe [a,c,****]

[a] Instituto de Física, Universidade de São Paulo, Rua do Matão, Travessa R, 187, CEP 05508-090, São Paulo, SP, Brazil
[b] Instituto do Mar, Universidade Federal de São Paulo, Rua Doutor Carvalho de Mendonça, 144, CEP 11070-100, Santos, SP, Brazil
[c] Instituto de Pesquisas Energéticas e Nucleares, IPEN-CNEN/SP, Av. Prof. Lineu Prestes, 2242, Cidade Universitária, 05508-000, São Paulo, SP, Brazil
[d] Escuela Profesional de Física, Facultad de Ciencias Naturales y Formales, Universidad Nacional de San Agustín de Arequipa (UNSA), Av. Independencia S/N, Arequipa, Peru

ARTICLE INFO

Keywords:
$CaSiO_3$
Defects centers
TL
EPR

ABSTRACT

β: $CaSiO_3$ polycrystal was synthesized by the devitrification method. The polycrystal exhibits three thermoluminescence (TL) peaks at 124 °C, 250 °C and 306 °C. Electron paramagnetic resonance (EPR) spectroscopy was used to study the defect centers induced in the polycrystal by gamma irradiation and to identify the centers responsible for the TL process. Three defect centers contribute to the observed spectrum at room temperature. Center I with principal *g*-values 2.0135, 2.0094 and 2.0038 is attributed to O^- ion and the center appears to be the recombination center for 124 °C, 147 °C and 306 C TL peaks. Center II exhibiting an isotropic *g*-value of 2.00025 is identified as an F^+-center (singly ionized oxygen vacancy). F^+-center is also observed to be a recombination center for several TL peaks. Center III is assigned to a Ti^{3+} center displaying an orthorhombic *g*-tensor with principal values $g_1 = 1.9830$, $g_2 = 1.9741$ and $g_3 = 1.9046$. This center is associated with 124 °C and 147 °C TL peaks. TL emission spectrum of β-$CaSiO_3$ shows two emission bands at 370 and 520 nm.

1. Introduction

Many natural and synthetic materials based on silica have been widely studied due to their applications which include radiation dosimetry using TL [1–5]. The defect centers created by ionizing radiation are responsible for TL. In this context, EPR spectroscopy provides a convenient and sensitive method to identify and characterize the defect centers in crystalline and amorphous materials [6–11], providing support in the identification of luminescent centers to understand the mechanisms of TL process. Therefore, luminescence studies must be combined with EPR for the full identification of the exact nature of the centers or defects responsible for the capture of the electrons. The knowledge of defects or traps and their distribution in the band gap of a solid are very essential in order to understand the luminescence process of materials and to use them in various applications.

The calcium metasilicate or also known as wollastonite ($CaSiO_3$) is an interesting material for study in mineralogy, either in its natural or synthetic form, due to the different polytypes described in many studies [12–14].

According to literature, natural and synthetic wollastonite can be classified by the formation conditions of pressure and temperature. In this way, three different structural modifications of wollastonite have been reported [12–14]. The low-temperature polymorphs are the triclinic wollastonite (1 T) and monoclinic wollastonite (2 M), the last one also known as parawollastonite. The high-temperature polymorph is a cyclosilicate called pseudowollastonite. Wollastonite polymorph (triclinic and monoclinic lattice) exist below about 1150 °C and contains single chains with three $[SiO_4]^{4-}$ tetrahedron as the repeat unit. In addition, the pseudowollastonite polymorph is stable above 1150 °C and melts at about 1550 °C with a structure containing rings of three silicates $(Si_3O_9)^{6-}$ [12,13].

Kulkarni et al. [15] reported EPR and photoluminescence studies on

* Corresponding author.
** Corresponding author.
*** Corresponding author.
**** Corresponding author. Instituto de Física, Universidade de São Paulo, Rua do Matão, Travessa R, 187, CEP 05508-090, São Paulo, SP, Brazil.
E-mail addresses: clorenzo@if.usp.br (C.D. Gonzales-Lorenzo), nilocano@if.usp.br (N.F. Cano), jayala@unsa.edu.pe (J.S. Ayala-Arenas), watanabe@if.usp.br (S. Watanabe).

https://doi.org/10.1016/j.jlumin.2019.116783
Received 16 July 2019; Received in revised form 23 September 2019; Accepted 26 September 2019
Available online 27 September 2019
0022-2313/© 2019 Elsevier B.V. All rights reserved.

$CaSiO_3$:Pb, Mn-nanophosphors which exhibits a broad resonance signal centered at $g = 1.994$ and an emission band at 353 nm in the UV region due to Pb^{2+}. Chakradhar et al. [16] have carried out EPR studies on Fe^{3+} - and Ni^{2+} - doped $CaSiO_3$. The EPR spectrum of Fe^{3+} ions in $CaSiO_3$ exhibits a weak signal at $g = 4.20 \pm 0.1$ and an intense signal at $g = 2.0 \pm 0.1$ while the spectrum of the Ni^{2+} ion exhibits a symmetric absorption at $g = 2.23 \pm 0.1$.

Palan et al. [17] studied the TL and optically stimulated luminescence (OSL) properties of $CaSiO_3$:Ce. They conclude that this material is a good alternative dosimeter compared to α-Al2O_3:C. Souza et al. [18] investigated the main features of the dosimeter of the Wollastnite-Teflon pellets. In this study, the authors show that the TL emission curve of the pellets is simple, has good response and reproducibility. Furthermore, its fading is minimal. Kulkarini et al. [19] studied the TL properties of β-$CaSiO_3$ nanophosphor under beta irradiation. They have observed that the TL intensity increases with radiation dose, a property desired by all TL dosimeters.

In recent years, defect centers in other silicate minerals, natural and synthetic, were investigated using the EPR technique in order to study their correlations with the peaks of the TL glow curve emission [8,9, 20–23].

As far as we know, no work has been published on the studies carried out on the role of defect centers in TL of the wollastonite. In this context, we perform EPR and TL studies of the synthetic wollastonaite irradiated with gamma rays and with different thermal treatments in order to identify the defect centers responsible for TL emission.

2. Experimental details

The synthetic $CaSiO_3$ polycrystal was produced by the devitrification method. In this work, we used 12.0 g (48.3 wt %) CaO and 12.8 g (51.7 wt %) of SiO_2 and the starting materials was mixed. The mixture is then placed in an oven heated to 1500 °C for 2 h. This flux melt is then cooled slowly so that the room temperature is reached after about 24 h to obtain polycrystalline material.

This polycrystalline sample of $CaSiO_3$ was crushed and sieved to retain grains 0.080–0.180 mm in size for TL and EPR measurements, while grains smaller than 0.080 mm in diameter were used in the structural analysis by X-rays diffraction (XRD) method.

TL measurements were carried out using Harshaw TL reader model 4500 in a nitrogen atmosphere; heating rate was kept at 4 °C/s. Luminescence was detected by a Hamamatsu R647 photomultiplier tube through a Schott KG1 filter (transmission band 330–690 nm). Five TL reading measurements were carried out to obtain an average TL glow curve. All TL readings were carried out 24 h after the irradiation took place, time enough to reach the stability of the TL peaks in $CaSiO_3$ polycrystals, except for the study of the fading of TL peaks at room temperature.

XRD data of powder sample at room temperature were obtained on Rigaku Miniflex 300 diffractometer with Cu $K_{\alpha 1}$ (0.15406 nm) radiation between 10° and 60° at a 0.02° (in 2θ) scanning step and a 1 s step time.

EPR measurements were performed at room temperature utilizing a MiniScope MS-5000 spectrometer from Freiberg Instruments. The EPR spectra were recorded at 9.45 GHz (X-band) microwave frequency, 20 mW microwave power, field modulation of 0.2 mT at 100 kHz, and a sweep time of 200 s. Three-accumulation scans were performed for each spectrum.

The irradiations for low dose of the order of mGy were done using a ^{137}Cs source of gamma rays and with a dose rate of 9.44 μGy/s at 30 cm from the source. For high doses in the region of hundreds of Gy and kGy were done using a ^{60}Co source type gamma-cell with a dose rate of 0.64 kGy/h, and a panoramic type source with a dose rate of 7.88 Gy/h at 40 cm from the source. The γ-irradiation was performed at room temperature and under conditions of electronic equilibrium.

3. Results and discussion

3.1. X-ray diffraction studies

The diffractogram of polycrystal sample is shown in Fig. 1. From the analysis of the diffractogram using computer software and compared with standard spectrum (PDF-2) of different crystals cataloged by ICDD (International Center for Diffraction Data), the peaks of the sample were identified as belonging to the principal phases of the pseudowollastonite (or β-$CaSiO_3$). This result shows that the devitrification method is adequate to obtain samples with a crystalline structure.

3.2. Thermoluminescence studies

β-$CaSiO_3$ sample exhibits TL peaks at approximately 124, 250, and 306 °C. The glow curves of β-$CaSiO_3$ sample irradiated with gamma low dose from 30 mGy to 500 mGy are shown in Fig. 2(a). Fig. 2(b), (c) and 2 (d) show the glow curves of β-$CaSiO_3$ sample irradiated with gamma ray dose from 1 to 10 Gy, 30 to 300 Gy and 500 to 50 kGy, respectively. This shows that the main glow peak is at 306 °C when irradiated from 30 mGy to 10 Gy and after that, the main glow peak at 250 °C becomes dominant due to the saturation of the TL peak at 306 for doses above 10 Gy.

Fig. 3 shows the TL response of the main TL peaks for dose ranging from 30 mGy to 50 kGy. Analyzing the dose-response curves with log axes on the same scale, as shown in Fig. 3, it can be observed that the TL response of all peaks at 124, 250 and 306 °C have a linear behavior in the dose range from about 30 mGy to 2.5 Gy. After that, TL responses are supralinear up to about 300 Gy for 124 and 306 °C TL peaks, and supralinear up to 3 kGy for 250 °C TL peak. Afterwards, all peaks are saturated.

With the purpose of finding the number and position as well as the activation energy of the TL peaks contained in the complex experimental glow curve of the β-$CaSiO_3$ polycrystals, the E-T_{stop} method was used [24,25].

Further, by the initial rise method it is possible to calculate the energy of the trap activation. This method is based on the fact that at low-temperature end of the peak, that is, the initial part of the TL glow curve can be well described by exponential behavior such as exp(-E/kT). Later, by the Arrhenius plot: ln(TL) vs 1/T which will be approximated as

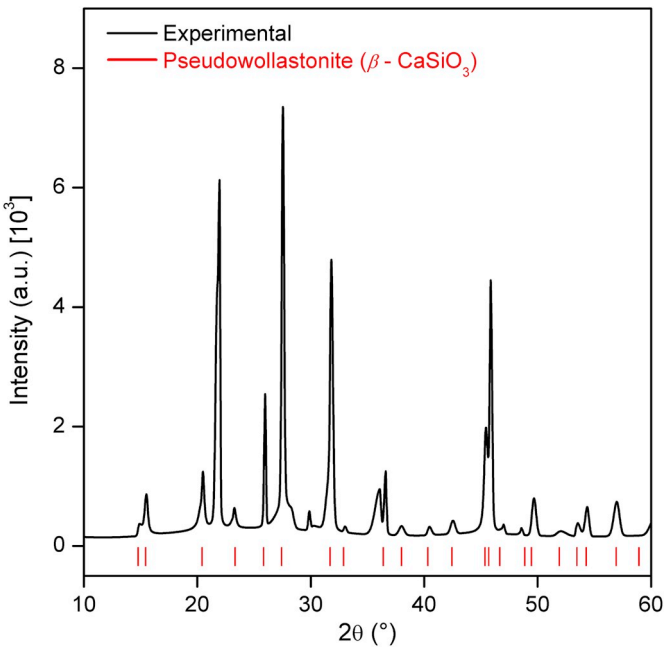

Fig. 1. X-ray diffraction of β-CaSiO3 produced in this work and the main pseudowollastonite diffraction peaks.

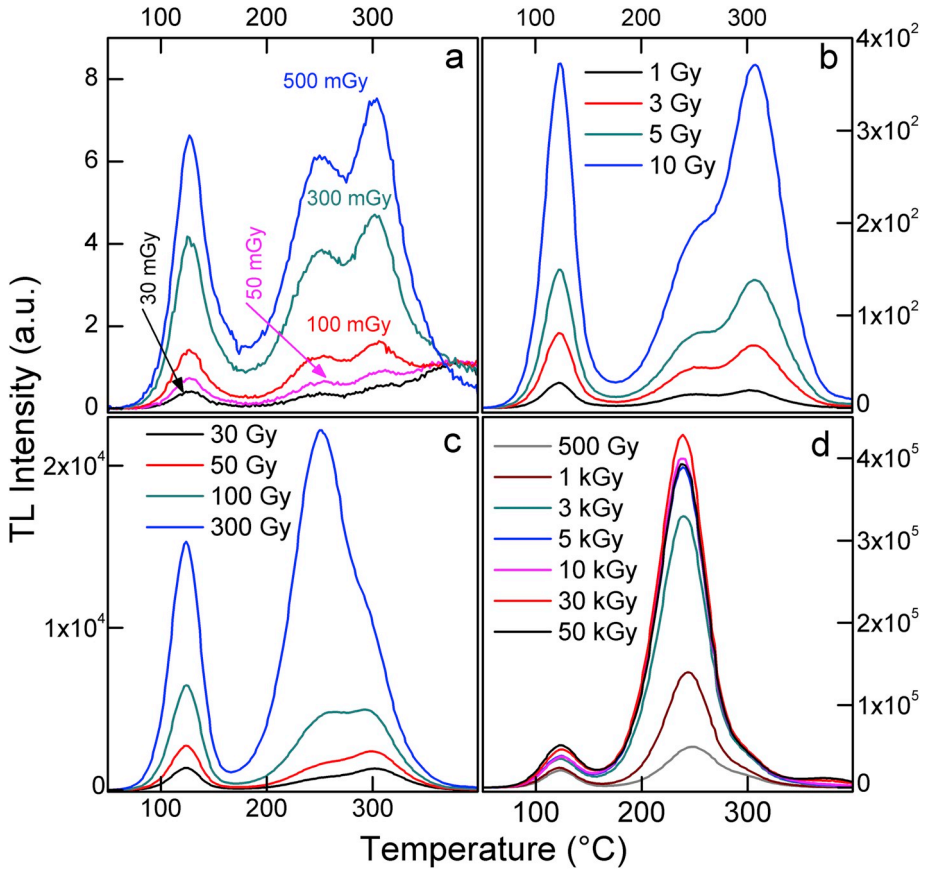

Fig. 2. TL Glow Curves of β-$CaSiO_3$, (a) irradiated with gamma rays low dose from 30 to 500 mGy, (b) from 1 to 10 Gy, (c) from 30 to 300 Gy, (d) from 500 Gy to 50 kGy. In all cases, a mass of about 1.93 mg was used.

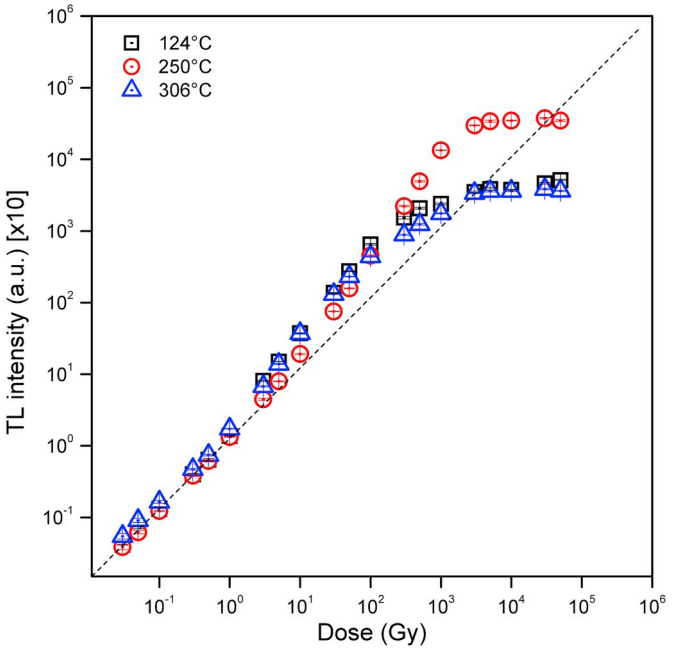

Fig. 3. TL intensity behavior of the 124, 250 and 306 °C peaks as a function of gamma radiation doses; dashed lines indicate linearity.

straight line, the activation energy E can be easily obtained from the slope $-E/k$. For a reliable result, it is only considered below 15% of the maximum TL intensity [26].

In this work, the activation energy was found using different pre-

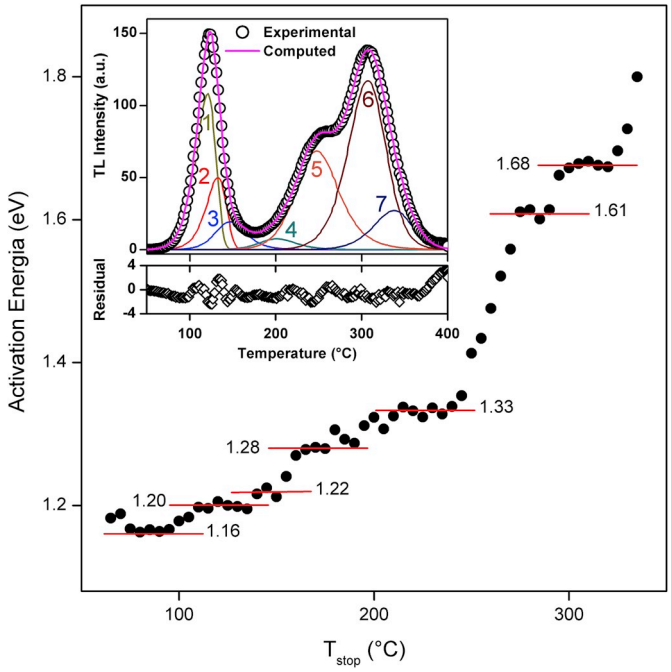

Fig. 4. Activation energy vs. T_{stop} method. In the inset, TL glow curve of β-$CaSiO_3$ irradiated with gamma dose of 5 Gy from ^{60}Co source. A good fit between the experimental glow curve (circles) and the simulated glow curve (pink line) can be achieved by assuming the presence of seven peaks. (For interpretation of the references to colour in this figure legend, the reader is referred to the Web version of this article.)

Table 1
Kinetic order, TL peak position, activation energy (E), frequency factor (s) of TL peaks of β-$CaSiO_3$ calculated by GCD. FOM = 1.335%.

Peak	Kinetic order	TL peak (°C)	E (eV)	s (s^{−1})	τ (years at 25 °C)
1	1st	121	1.16	2.40×10^{14}	0.005
2	1st	133	1.2	2.69×10^{14}	0.023
3	2nd	147	1.22	1.39×10^{14}	0.095
4	2nd	201	1.28	1.07×10^{13}	12.80
5	2nd	247	1.33	1.77×10^{12}	543.8
6	1.5	306	1.61	2.27×10^{13}	2292×10^{3}
7	1.4	336	1.68	1.62×10^{13}	3929×10^{4}

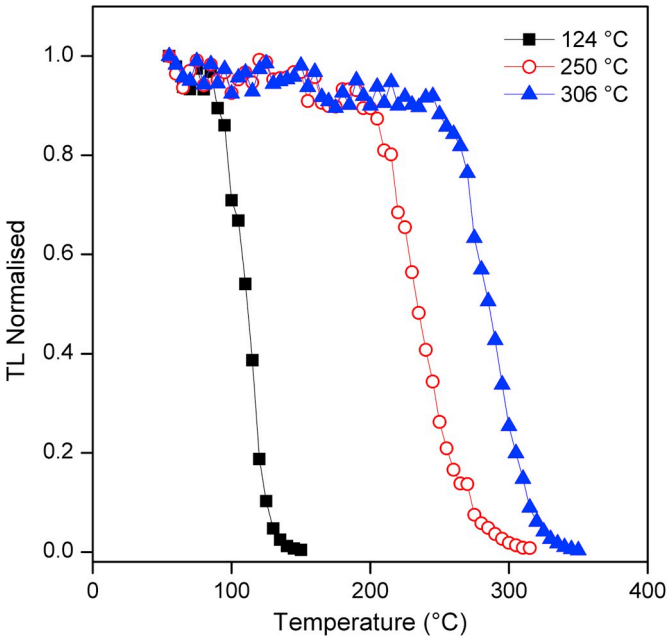

Fig. 5. Thermal stabilities of main TL peaks at 124, 250 and 306 °C.

heating temperature (T_{stop}) from 60 to 330 °C at a 5 °C scanning step. Fig. 4 shows the obtained activation energies (E) using the E-T_{stop} method for β-$CaSiO_3$ samples.

Another broadly used method is the glow-curve deconvolution (GCD) to compute characteristics parameters like E, s and the order of the kinetic (b) of individual glow peaks on the experimental TL glow curve [27].

The position of the first peak is the same with increasing doses. In this way, a first-order peak will be more appropriate. For the second peak, however, the peak shift to lower temperature with increasing doses as shown in Fig. 2(d). Therefore, this peak is considered as a second-order peak. The third peak shows a better fitting with a general-order kinetic. Therefore, using the previous results found by the E-T_{stop} method and applying the equation proposed by Kitis et al. [27] we obtain the deconvolution of the TL glow curve of the β-$CaSiO_3$ sample irradiated with gamma dose of 5 Gy (see Fig. 4).

The TL glow curves in Fig. 2 present three well-defined peaks and the GCD method shows seven overlapping TL peaks. The inset of Fig. 4 shows these computed TL peaks separated using different orders of kinetics at about 121, 133, 147, 201, 247, 306 and 337 °C. Quality of fit was tested with the Figure of Merit (FOM) [28]. FOM = 1.335% shows that data fit is satisfactory.

The position, activation energies (E) and frequency factor (s) of the TL peaks of β-$CaSiO_3$ sample are shown in Table 1. The thermal stabilities of main TL peaks at 124, 250 and 306 °C are shown in Fig. 5.

Anomalous fading is an important characteristic of natural and synthetic crystalline materials [25]. For this purpose, β-$CaSiO_3$ sample

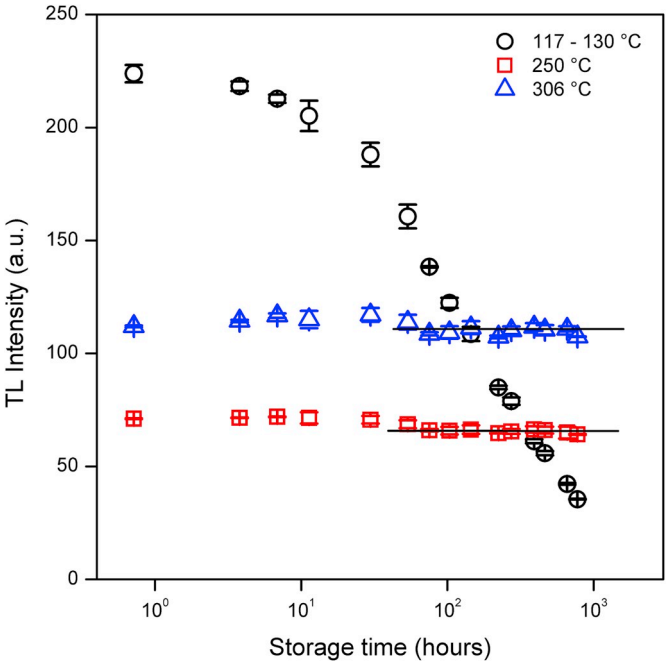

Fig. 6. TL intensity of the β-$CaSiO_3$ samples irradiated with 5 Gy against the storage time at room temperature.

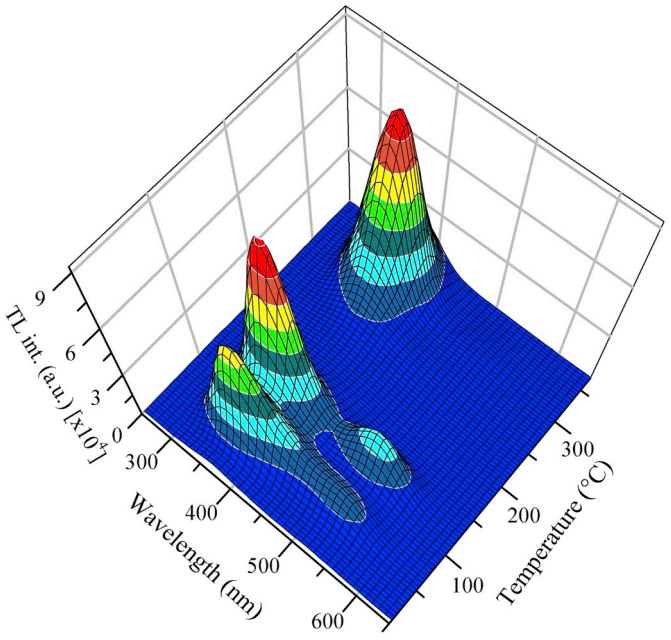

Fig. 7. TL spectra of β-$CaSiO_3$ sample after beta irradiation dose of 12.2 Gy.

was irradiated with 5 Gy gamma dose and kept in the dark at room temperature for different storage time. Its TL was read after 1, 3, 6, etc. hours up to about 32 days (775 h). Fig. 6 shows the results of fading for TL peaks at 117–130, 250, and 306 °C. The TL peak at 117 °C is a low-temperature peak and is commonly unstable at room temperature and decays by about 84% after 32 days storage time. TL peak at 250 and 306 °C are the high-temperature peaks having a decay of about 7% and 3% respectively in the first 48 h, after that time, there is no decay.

The TL emission spectrum of the polycrystal β-$CaSiO_3$ presented two very broad bands centered at 370 and 520 nm (Fig. 7). This means that one should expect two recombination centers. TL glow curves with the emission in the region 370 nm show TL peaks at around 70, 140 and

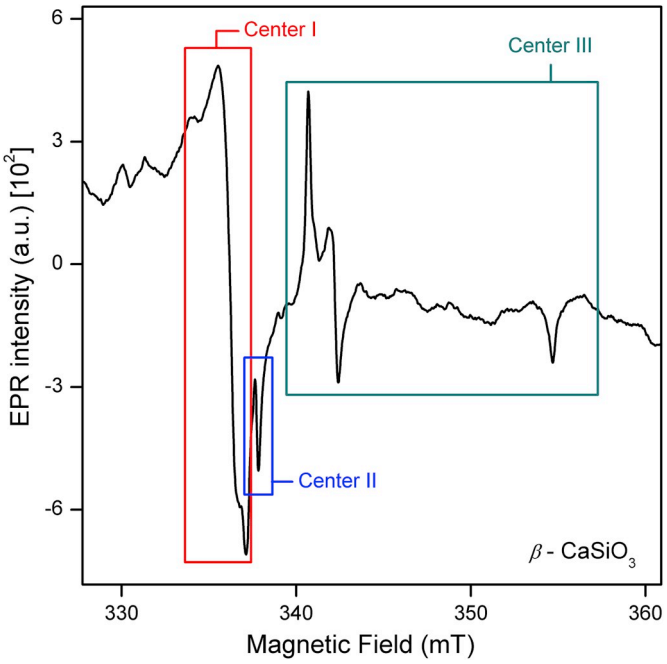

Fig. 8. Room temperature EPR spectra of irradiated β-$CaSiO_3$ (gamma dose: 6 kGy). The line labeled as I is due to an O^- ion and center II line is from an F^+ -center. The Ti^{3+} -center is indicated as center III.

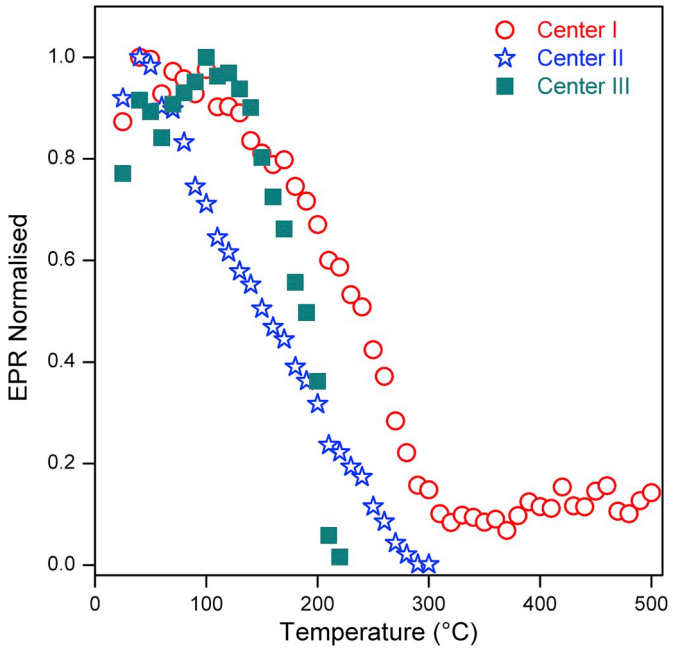

Fig. 9. Thermal annealing behavior of Center I (O^- ion), Center II (F^+ center) and Center III (Ti^{3+} center) in β-$CaSiO_3$ (pseudowollastonite). The intensity was normalized by the maximum value of the EPR signal for each center.

306 °C, whereas that emission band at 520 nm corresponds to two TL peaks at approximately 70 and 135 °C. It is important to mention that the peak around 70 °C shown in Fig. 7 decays completely in a few minutes than the other peaks. In the emission spectrum TL of Fig. 7, TL peaks are observed at approximately 70 °C as measurement of the TL emission curve was done immediately after irradiation.

3.3. Electron paramagnetic resonance studies

The room temperature EPR spectrum of gamma irradiated (dose: 6 kGy) β-$CaSiO_3$ is shown in Fig. 8. It is inferred from thermal annealing studies that three different centers contribute to the observed spectrum. The centers are labeled in Fig. 8.

In a perfect β-$CaSiO_3$ lattice, Ca and Si atoms are expected to be situated in their respective sites. However, antisite cation exchange may be present resulting in partial replacement of Ca atoms by Si atoms. This exchange called as cation exchange disorder is a point defect in crystal lattices where cations exchange positions. Kuklja [29] has predicted the presence of such defects based on theoretical calculations. This prediction is supported by X-ray diffraction [30] and X-ray absorption fine structure studies [31]. It has also been possible to directly observe these defects using advanced electron microscopy [32].

The line labeled as center I in Fig. 8 is characterized by a rhombic g-tensor with principal values $g_1 = 2.0135$, $g_2 = 2.0094$ and $g_3 = 2.0038$. The linewidth of the line corresponding to $g = 2.0094$ is about 12 Gauss (1.2 mT). The EPR line is broad and could arise from a possible unresolved hyperfine structure. The unresolved structure can arise from the interaction of the unpaired electron with nearby nuclear spins. Calcium and silicon in $CaSiO_3$ have isotopes with nuclear spins 7/2 and 1/2 (^{49}Ca and ^{29}Si respectively) [33]. It is possible that the electronic spin will interact with Ca ions and also with Si ions. In $CaSiO_3$, a number of lattice defects may form due to non-stoichiometry and cation disorder mentioned earlier. First principle calculations suggest that the possibility of formation of oxygen vacancies is high in a lattice with antisite cation disorder [34]. F^+-center will form easily in a lattice with cation disorder by trapping electrons at oxygen vacancies. On the other hand, calcium and silicon vacancies can trap holes and form V-centers or O^- ions [35]. The relatively broad line of center I arising from unresolved hyperfine structure indicates the delocalization of the unpaired electron and an interaction with nearby nuclei. It has been suggested that in oxides [36] charges must be trapped near double or more charged defects allowing the charge to be delocalized and interact with nearby nuclei. The observed magnitude of g-values and the large orthorhombicity of g-tensor are characteristic of an O^- ion which results from capture of a hole at O^{2-} ions. Examples are O^- ion observed in systems like $KNbO_3$ [37] and $SrTiO_3$ [38]. The hole resides in O^- (2p) orbital resulting in one of the principal g-value close to free-spin value. On the basis of these observations, center I in $CaSiO_3$ is tentatively attributed to an O^- ion. The thermal annealing behavior of center I is shown in Fig. 9. It is observed that the center decays in the broad temperature range starting from about 50 °C to 290 °C. It is speculated that the decay extends a little beyond 290 °C and the spectrometer may not have sensitivity to detect this weak signal. As the decay of the center extends over a range of TL peaks, it is suggested that center I (O^- ion) could be the recombination center for TL peaks at 124 °C, 147 °C and 306 C. The thermal stabilities of individual dominant TL peaks are shown in Fig. 5. This behavior of TL peaks indicates that neither center I or II can be associated exclusively with an individual TL peak. Rather it appears that center I is the recombination center for multiple TL peaks.

The EPR line labeled as center II in Fig. 8 has an isotropic g-value of 2.00025 and a linewidth of 2 G (0.2 mT). Oxygen vacancies present in the lattice due to reasons mentioned earlier can trap electrons and form F^+-centers. Earlier observation of this center is in LiF [39] where the center exhibited a very large linewidth and a g-value close to free-electron value. The inherent linewidth of F^+-center is very small (~1G) as observed in MgO [40]. Amount of delocalization of the unpaired electron decides the linewidth along the magnetic moment and relative abundance of the isotopes of the ions. In alkali halides, electron is observed to be considerably delocalized and F^+-center in these systems exhibit large linewidths. For example, linewidth of 58 G and 20 G are observed in LiCl and KCl, respectively [41]. On the other hand, the center in BaO has a small linewidth of 3.5 G [42]. Apart from alkali halides, F^+-center can form in oxide systems. In both alkali halides and oxides, the g-value has been found to be close to free-electron value with g-shifts being either positive or negative. In β-wollastonite, the linewidth

is not large and the *g*-shift is small. On the basis of these observations, center II is tentatively identified as an F^+-center. Fig. 9 shows the thermal annealing results of center II. It is seen that the intensity of EPR line decreases in the temperature range from about 70 °C to 300 °C. It is observed that the decay temperature range of center II is almost the same as center I. This behavior compels us to speculate that this center is also associated with 124 °C, 147 °C and 306 °C TL peaks and perhaps is also a recombination center for all these peaks. Center II line intensity is quite small and as with center I may completely decay at a temperature which is slightly higher than 300 °C.

EPR line labeled as center III in Fig. 8 originates from a single defect center displaying an orthorhombic *g*-tensor with principal values $g_1 = 1.9830$, $g_2 = 1.9741$ and $g_3 = 1.9046$. The center is seen to exhibit relatively large *g*-anisotropy and the principal values are similar to Ti^{3+} center [43]. It is speculated that titanium ion is present in $CaSiO_3$ as an impurity and incorporated into the lattice during synthesis of $CaSiO_3$. Large *g*-shifts are expected for the Ti^{3+} center as the spin-orbit coupling of titanium ion is high ($\lambda = 154\ cm^{-1}$: free-ion value). The first observation on Ti^{3+} center was in X-irradiated rose quartz by Wright et al. [43]. In rose quartz, centers arise from titanium ion located substitutionally at silicon sites. Two sets of lines were observed and both were assigned to Ti^{3+} centers. Wright et al. [43] attributed the centers to Ti^{3+} centers based on the weak anisotropic hyperfine structure coming from low abundance odd titanium isotopes namely, ^{47}Ti and ^{49}Ti. On the basis of the experimentally observed orientation of the principal *g*-axes and from the fact that titanium forms tetrahedral compounds, it was suggested that titanium has substituted silicon atoms. It was further suggested that the titanium center is formed from the capture of an electron, released due to X-irradiation, on the titanium central atom located at the center of a distorted tetrahedron in α-quartz.

Several Ti centers have been observed in silicate minerals and $CaSiO_3$ is also a silicate system. Ding et al. [44] have shown in a theoretical study that Ti^{3+} ion located in an orthorhombically elongated tetrahedral $[TiO_4]^{5-}$ cluster on W^{6+} site in $ZnWO_4$ is characterized by the principal *g*-values 1.967, 1.955 and 1.989. The experimentally observed *g*-values in $ZnWO_4$ are 1.843, 1.895 and 1.933 [45]. In another case of Ti^{3+} ions at a low symmetry tetrahedral Si^{4+} site in Beryl ($Be_3Al_2Si_6O_{18}$), Yang et al. [46] have calculated the principal *g*-values to be 1.998, 1.917 and 1.875. In an EPR study on Beryl, the experimentally observed values are 1.998, 1.907 and 1.866 [47]. On the basis of these theoretical and experimental results, center III in $CaSiO_3$ is tentatively attributed to a Ti^{3+} center. Titanium impurity ions are located at Si sites in $CaSiO_3$. They capture an electron during irradiation resulting in the formation of Ti^{3+} center.

Fig. 9 shows the thermal annealing behavior of center III. It is observed that the center becomes unstable around 110 °C and decays in the temperature range 110 °C–210 °C. This decay relates to the 147 °C TL peak and perhaps also with the 124 °C peak.

4. Conclusions

β-$CaSiO_3$ sample of the calcium silicate polycrystal exhibits TL peaks at 124 °C, 250 °C and 306 °C. This material shows a broad range dosimetric capability to low gamma radiation dose of the order of 30 mGy and to high doses in the region of kGy. Thermal fading for β-$CaSiO_3$ have shown an unstable low-temperature peak but stable high-temperature peaks which decay about 7% in the first 48 h, but after that, there is no decay up to 32 days. Furthermore, the high luminescent sensitivity shown by this synthetic sample to gamma radiation dose make it an interesting material for applications in radiation dosimetry.

The TL spectra emission of the β-$CaSiO_3$ presents a very intense 370 nm band and a weak 520 nm band. This result shows that β-$CaSiO_3$ polycrystal has in principle two recombination centers that participate in TL process. The electron transition responsible for these emission lines will be the main aim of study in a near future.

Three defect centers are observed in β-$CaSiO_3$ and these are tentatively attributed to an O^- ion, F^+-center, and Ti^{3+} center. O^- ion and F^+-center seem to be the recombination centers associated with 124 °C, 147 °C and 306 °C TL peaks. Ti^{3+}center is related to 154 °C and also possibly with the 124 °C TL peak.

Acknowledgements

The authors wish to thank Ms. E. Somessari and Mr. Aldo Oliveira, Institute for Energy and Nuclear Researches (IPEN), Brazil, for kindly carrying out the irradiation of the samples. To FAPESP (Process number 2014/03085-0) for partial financial support and to CNPq for fellowship to C.D. Gonzales-Lorenzo (Process number 162741/2015-4).

References

[1] N.F. Cano, J.M. Yauri, S. Watanabe, J.C.R. Mittani, A.R. Blak, Thermoluminescence of natural and synthetic diopside, J. Lumin. 128 (2008) 1185–1190. https://doi.org/10.1016/j.jlumin.2007.11.090.
[2] W. Shigueo, N.F. Cano, T.K. Gundu Rao, L.M. Oliveira, L.S. Carmo, J.F.D. Chubaci, Radiation dosimetry using decreasing TL intensity in a few variety of silicate crystals, Appl. Radiat. Isot. 105 (2015) 119–122. https://doi.org/10.1016/j.apradiso.2015.07.056.
[3] R.F. Barbosa, N.F. Cano, S. Watanabe, R.A.S. Guttler, F. Reichmann, Thermoluminescence in two varieties of jadeite: irradiation effects and application to high dose dosimetry, Radiat. Meas. 71 (2014) 36–38. https://doi.org/10.1016/j.radmeas.2014.05.002.
[4] S. Watanabe, N.F. Cano, L.S. Carmo, R.F. Barbosa, J.F.D. Chubaci, High- and very-high-dose dosimetry using silicate minerals, Radiat. Meas. 72 (2015) 66–69. https://doi.org/10.1016/j.radmeas.2014.11.004.
[5] C.D. Gonzales-Lorenzo, S. Watanabe, N.F. Cano, J.S. Ayala-Arenas, C.C. Bueno, Synthetic polycrystals of $CaSiO_3$ un-doped and Cd, B, Dy, Eu-doped for gamma and neutron detection, J. Lumin. 201 (2018) 5–10. https://doi.org/10.1016/j.jlumin.2018.04.037.
[6] N.F. Cano, L.H.E. Santos, J.F.D. Chubaci, S. Watanabe, Study of luminescence, color and paramagnetic centers properties of albite, Spectrochim. Acta A 137 (2015) 471–476. https://doi.org/10.1016/j.saa.2014.08.085.
[7] E.A. Gallegos, N.F. Cano, S. Watanabe, J.F.D. Chubaci, Thermoluminescence, infrared reflectivity and electron paramagnetic resonance properties of hemimorphite, Radiat. Meas. 44 (2009) 11–17. https://doi.org/10.1016/j.radmeas.2008.10.003.
[8] N.F. Cano, A.R. Blak, S. Watanabe, Correlation between electron paramagnetic resonance and thermoluminescence in natural sodalite, Phys. Chem. Miner. 37 (2010) 57–64. https://doi.org/10.1007/s00269-009-0309-z.
[9] N.F. Cano, A.R. Blak, J.S.A. Arenas, S. Watanabe, Mechanisms of TL for production of the 230°C peak in natural sodalite, J. Lumin. 131 (2011) 165–168. https://doi.org/10.1016/j.jlumin.2010.09.027.
[10] N.O. Dantas, W.E.F. Ayta, A.C.A. Silva, N.F. Cano, A.F.R. Rodriguez, A. Oliveira, V. Garg, P.C., Morais Magnetic and optical investigation of $40SiO_2{\cdot}30Na_2O{\cdot}1Al_2O_3{\cdot}(29 - x)B_2O_3{\cdot}xFe_2O_3$ glass matrix, Solid State Sci. 14 (2012) 1169–1174. https://doi.org/10.1016/j.solidstatesciences.2012.05.033.
[11] R.S. Silva, J.T.T. Silva, V.R. Rocha, N.F. Cano, A.C.A. Silva, N.O. Dantas, Synthesis process controlled of semimagnetic $Bi_{2-x}Mn_xS_3$ nanocrystals in a host glass matrix, J. Phys. Chem. C 118 (2014) 18730–18735. https://doi.org/10.1021/jp5046657.
[12] W.A. Deer, R.A. Howie, J. Zussman, An Introduction to the Rock-Forming Minerals, second ed., Longman, England, 1992.
[13] E. Mazzucato, A.F. Gualtieri, Wollastonite polytypes in the CaO-SiO_2 system, Phys. Chem. Miner. 27 (2000) 565–574. https://doi.org/10.1007/s002690000095.
[14] K. Hesse, Refinement of the crystal structure of wollastonite-2M (parawollastonite), Z. Krist-Cryst Mater. 168 (1984) 93–98. https://doi.org/10.1524/zkri.1984.168.14.93.
[15] S. Kulkarni, B.M. Nagabhushana, N. Suriyamurthy, C. Shivakumara, R.P. S. Chakradhar, R. Damle, Synthesis, luminescence and EPR studies on $CaSiO_3$: Pb, Mn-nanophosphors synthesized by the solution combustion method, Ceram. Int. 39 (2013) 1917–1922. https://doi.org/10.1016/j.ceramint.2012.08.041.
[16] R.P.S. Chakradhar, B.M. Nagabhushana, G.T. Chandrappa, J.L. Rao, K.P. Ramesh, EPR study of Fe^{3+}- and Ni^{2+}-doped macroporous $CaSiO_3$, Appl. Magn. Reson. 137 (2008) 33. https://doi.org/10.1007/s00723-008-0060-5.
[17] C.B. Palan, K.A. Koparkar, N.S. Bajaj, S.K. Omanwar, Synthesis and TL/OSL properties of $CaSiO_3$:Ce biomaterial, Mater. Lett. 175 (2016) 288–290. https://doi.org/10.1016/j.matlet.2016.04.006.
[18] D.N. Souza, A.P. Melo, L.V.E. Caldas, TL and TSEE response of Wollastonite-Teflon composites in X-ray beams, Nucl. Instrum. Methods A 580 (2007) 338–341. https://doi.org/10.1016/j.nima.2007.05.170.
[19] S. Kulkarni, B.M. Nagabhushana, H. Nagabhushana, K.V.R. Murthy, C. Shivakumara, R. Damle, Synthesis, structural characterization and thermoluminescence properties of β-Irradiated Wollastonite Nanophosphor, Trans. Indian Ceram. Soc. 70 (2011) 163–166. https://doi.org/10.1080/0371750X.2011.10600165.
[20] N.F. Cano, T.K. Gundu, C.D. Gonzales-Lorenzo, J.S. Ayala-Arenas, H.S. Javier-Ccallata, S. Watanabe, Thermoluminescence and defect centers in synthetic diopside, J. Lumin. 211 (2019) 314–319. https://doi.org/10.1016/j.jlumin.2019.03.038.

[21] N.F. Cano, T.K. Gundu Rao, J.S. Ayala-Arenas, C.D. Gonzales-Lorenzo, L. M. Oliveira, S. Watanabe, TL in green tourmaline: study of the centers responsible for the TL emission by EPR analysis, J. Lumin. 205 (2019) 324–328. https://doi.org/10.1016/j.jlumin.2018.09.034.
[22] N.B. Silva-Carrera, N.F. Cano, T.K. Gundu Rao, J.S. Ayala-Arenas, S. Watanabe, Thermoluminescence in Lapis Lazuli crystal: glow peaks and their connection with F-centers estimated by ESR analysis, J. Lumin. 188 (2017) 472–477. https://doi.org/10.1016/j.jlumin.2017.04.057.
[23] T.K. Gundu Rao, N.F. Cano, B.N. Silva-Carrera, R.M. Ferreira, H.S. Javier-Ccallata, S. Watanabe, Centers responsible for the TL peaks of willemite mineral estimated by EPR analysis, J. Lumin. 177 (2016) 139–144. https://doi.org/10.1016/j.jlumin.2016.04.026.
[24] S.W.S. McKeever, On the analysis of complex thermoluminescence glow-curves: resolution into individual peaks, Phys. Status Solidi 62 (1980) 331–340. https://doi.org/10.1002/pssa.2210620139.
[25] R. Chen, S.W.S. McKeever, Theory of Thermoluminescence and Related Phenomena, World Scientific, 1997.
[26] P. Kivits, H.J.L. Hagebeuk, Evaluation of the model for thermally stimulated luminescence and conductivity; reliability of trap depth determinations, J. Lumin. 15 (1977) 1–27. https://doi.org/10.1016/0022-2313(77)90002-3.
[27] G. Kitis, J.M. Gomez-Ros, W.N. Tuyn, Thermoluminescence glow-curve deconvolution functions for first, second and general orders of kinetics, J. Phys. D Appl. Phys. 31 (1998) 2636–2641. https://doi.org/10.1088/0022-3727/31/19/037.
[28] H.G. Balian, N.W. Eddy, Figure-of-Merit (FOM), an improved criterion over the normalized chi-squared test for assessing goodness-of-fit of gamma-ray spectral peaks Nucl, Instrum. Methods 145 (1977) 389–395. https://doi.org/10.1016/0029-554X(77)90437-2.
[29] M.M. Kuklja, Defects in yttrium aluminium perovskite and garnet crystals: atomistic study, J. Phys. Condens. Matter 12 (2000) 2953–2967. https://doi.org/10.1088/0953-8984/12/13/307.
[30] A.P. Patel, M.R. Levy, R.W. Grimes, R.M. Gaume, R.S. Frigelson, K.J. McClellan, C. R. Stanek, Mechanisms of nonstoichiometry in $Y_3Al_5O_{12}$, Appl. Phys. Lett. 93 (2008), 191902-191902-3, https://doi.org/10.1063/1.3002303.
[31] J. Dong, K. Lu, Noncubic symmetry in garnet structures studied using extended X-ray-absorption fine-structure spectra, Phys. Rev. B 43 (1991) 8808–8821. https://doi.org/10.1103/PhysRevB.43.8808.
[32] D. Truong, M.K. Devaraju, T. Tomai, I. Honma, Direct observation of antisite defects in $LiCoPO_4$ cathode materials by annular dark- and bright-field electron microscopy, ACS Appl. Mater. Interfaces 5 (2013) 9926–9932. https://doi.org/10.1021/am403018n.
[33] R.C. Weast (Ed.), Handbook of Chemistry and Physics, CRC, Cleveland, 1971.
[34] N. Yuan, X. Liu, F. Meng, D. Zhou, J. Meng, First-principles study of La_2CoMnO_6: a promising cathode material for intermediate-temperature solid oxide fuel cells due to intrinsic Co-Mn cation disorder, Ionics 21 (2015) 1675–1681. https://doi.org/10.1007/s11581-014-1320-z.
[35] M.S. Holston, J.W. McClory, N.C. Giles, L.E. Halliburton, Radiation-induced defects in $LiAlO_2$ crystals: holes trapped by lithium vacancies and their role in thermoluminescence, J. Lumin. 160 (2015) 43–49, 2015, https://doi.org/10.1016/j.jlumin.2014.11.018.
[36] N.Y. Konstantinov, L.V. Karaseva, V.V. Gromov, Dokl. Akad. Nauk SSSR 228 (1980) 631.
[37] E. Possenriede, B. Hellermannand, O.F. Schirmer, O^- trapped holes in acceptor doped KNbO3, Solid State Commun. 65 (1988) 31–33. https://doi.org/10.1016/0038-1098(88)90581-9.
[38] O.F. Schirmer, W. Berlinger, K.A. Muller, Holes trapped near Mg^{2+} and Al^{3+} impurities in SrTiO3, Solid State Commun. 18 (1976) 1505–1508. https://doi.org/10.1016/0038-1098(76)90380-X.
[39] C.A. Hutchison, Paramagnetic resonance absorption in crystals colored by irradiation, Phys. Rev. 75 (1949) 1769–1770. https://doi.org/10.1103/PhysRev.75.1769.2.
[40] J.E. Wertz, P. Auzins, R.A. Weeks, R.H. Silsbee, Electron spin resonance of F centers in magnesium oxide; confirmation of the spin of magnesium-25, Phys. Rev. 107 (1957) 1535–1537. https://doi.org/10.1103/PhysRev.107.1535.
[41] W.C. Holton, H. Blum, Paramagnetic resonance of F centers in alkali halides, Phys. Rev. 125 (1962) 89–103. https://doi.org/10.1103/PhysRev.125.89.
[42] A.J. Tench, R.L. Nelson, Electron spin resonance of F centres in irradiated ^{43}CaO and other alkaline earth oxides, Proc. Phys. Soc. 92 (1967) 1055–1063. https://doi.org/10.1088/0370-1328/92/4/328.
[43] P. M Wright, J.A. Weil, T. Buch, J.H. Anderson, Titanium colourcentres in rose quartz, Nature 197 (1963) 246–248. https://doi.org/10.1038/197246a0.
[44] C.C. Ding, S. Wu, Q. Zhu, Z. Zhang, B. Teng, M. Wu, An investigation on the defect structures and spin Hamiltonian parameters for the two orthorhombic Ti³⁺ centers in $ZnWO_4$, J. Phys. Chem. Solids 86 (2015) 141–147. https://doi.org/10.1016/j.jpcs.2015.06.017.
[45] A. Watterich, A. Hofstaetter, R. Wuerz, A. Scharmann, Ti³⁺centres in reduced $ZnWO_4$:Ti single crystals, Solid State Commun. 100 (1996) 513–518. https://doi.org/10.1016/0038-1098(96)00435-8.
[46] M. Yang, W. Xiao-Xuan, Z. Wen-Chen, EPR parameters and defect structure of the tetrahedral Ti³⁺ defect center in beryl crystal, Radiat. Eff. Defects Solids 163 (2008) 79–83. https://doi.org/10.1080/10420150701259214.
[47] V.P. Solntsev, A.M. Yurkin, Valence states and coordination of titanium ions in beryl crystals, Crystallogr. Rep. 45 (2000) 128–132. https://doi.org/10.1134/1.171148.